American Mineralogist, Volume 76, pages 493–500, 1991

Calcium depletion halos and Fe-Mn-Mg zoning around faceted plagioclase inclusions in garnet from a high-grade pelitic gneiss

Donna L. Whitney
Department of Geological Sciences, AJ-20, University of Washington, Seattle, Washington 98195, U.S.A.

Abstract

Faceted, reversely zoned plagioclase inclusions surrounded by Ca depletion halos and Fe-Mg-Mn zoning in garnet are present in sillimanite-bearing rocks from the Skagit Gneiss in the North Cascade Range of Washington. Garnets are homogeneous except near the rim and near plagioclase inclusions. In the vicinity of plagioclase inclusions, the grossular component of garnet decreases by 2–8 mol%, almandine increases by 4–10 mol%, pyrope decreases by 1–13 mol%, and spessartine increases by <1–4 mol% from the average core composition. The observations (1) that garnet is zoned around plagioclase inclusions, (2) that zoning is most pronounced around inclusions in pervasively fractured garnets, and (3) that the extent of garnet zoning around each inclusion is related to the location of fractures are evidence for chemical communication between plagioclase inclusions and matrix phases.

The facets of the plagioclase inclusions are garnet crystal faces. All inclusions are reversely zoned; anorthite content increases by 12–24 mol% from core to rim. Zoning parallels the plagioclase-garnet interface of both negative crystals and irregularly shaped inclusions, suggesting that zoning is not a preentrapment feature.

These observations demonstrate that postentrapment changes in plagioclase inclusions can occur during evolving *P-T* conditions. This possibility must be considered when using the composition of plagioclase inclusions in garnet for geobarometric calculations and quantitative *P-T* path construction.

Introduction

Biotite inclusions in garnets in middle- and high-grade metamorphic rocks are typically affected by Fe-Mg exchange reaction with the surrounding host during retrograde metamorphism. In contrast, however, it is usually inferred that plagioclase inclusions in garnet preserve equilibrium compositions attained at peak metamorphic temperatures because net transfer involving additional phases is required to balance the garnet-plagioclase reaction stoichiometry (Spear, 1989).

The composition of plagioclase inclusions in garnet is commonly used with garnet core compositions for geobarometric calculations of peak metamorphic pressures and is combined with information from garnet zoning in the construction of *P-T* paths (Spear and Selverstone, 1983; Spear and Rumble, 1986). This technique has been successfully applied to rocks in which the anorthite content of plagioclase inclusions varies systematically from garnet core to rim and when inclusion compositions can be matched with the anorthite content of zoned matrix plagioclase (St. Onge, 1987).

Ca depletion halos surrounding plagioclase inclusions in garnet have been observed in sillimanite + potassium feldspar rocks (5–6 kbar, 725 °C) and attributed to postentrapment reaction with other inclusions in garnet (Lieberman, 1988). Loomis (1983), however, noted that inclusions in garnet may not be chemically isolated from matrix phases if cracks are present and cautioned that diffusion halos around inclusions might not be resolvable by microprobe analysis. The purpose of the present study is to document an example of well-developed halos around plagioclase inclusions in garnets in a high-grade pelitic gneiss and to demonstrate that postentrapment changes in inclusion composition are related to fractures in the host garnet. These observations have implications for the use of plagioclase inclusions in geobarometry and *P-T* path calculations.

Metamorphic history

The rocks examined in this study are from an outcrop of migmatitic sillimanite gneiss from the upper amphibolite-facies Skagit Gneiss, North Cascades. These rocks contain biotite, plagioclase, quartz, garnet, sillimanite (some as fibrous sillimanite), ilmenite, cordierite, iron sulfide, zircon, and apatite. Cordierite is not a matrix phase, but cordierite-quartz intergrowths are present in some garnet cores that have been partially replaced by plagioclase and biotite. Kyanite and rutile are present as inclusions in garnet.

The maximum *P-T* conditions recorded by pelitic rocks in the Skagit Gneiss are 9–10 kbar and 700–725 °C, and the decompression path is interpreted to have been nearly

0003–004X/91/0304–0493$02.00

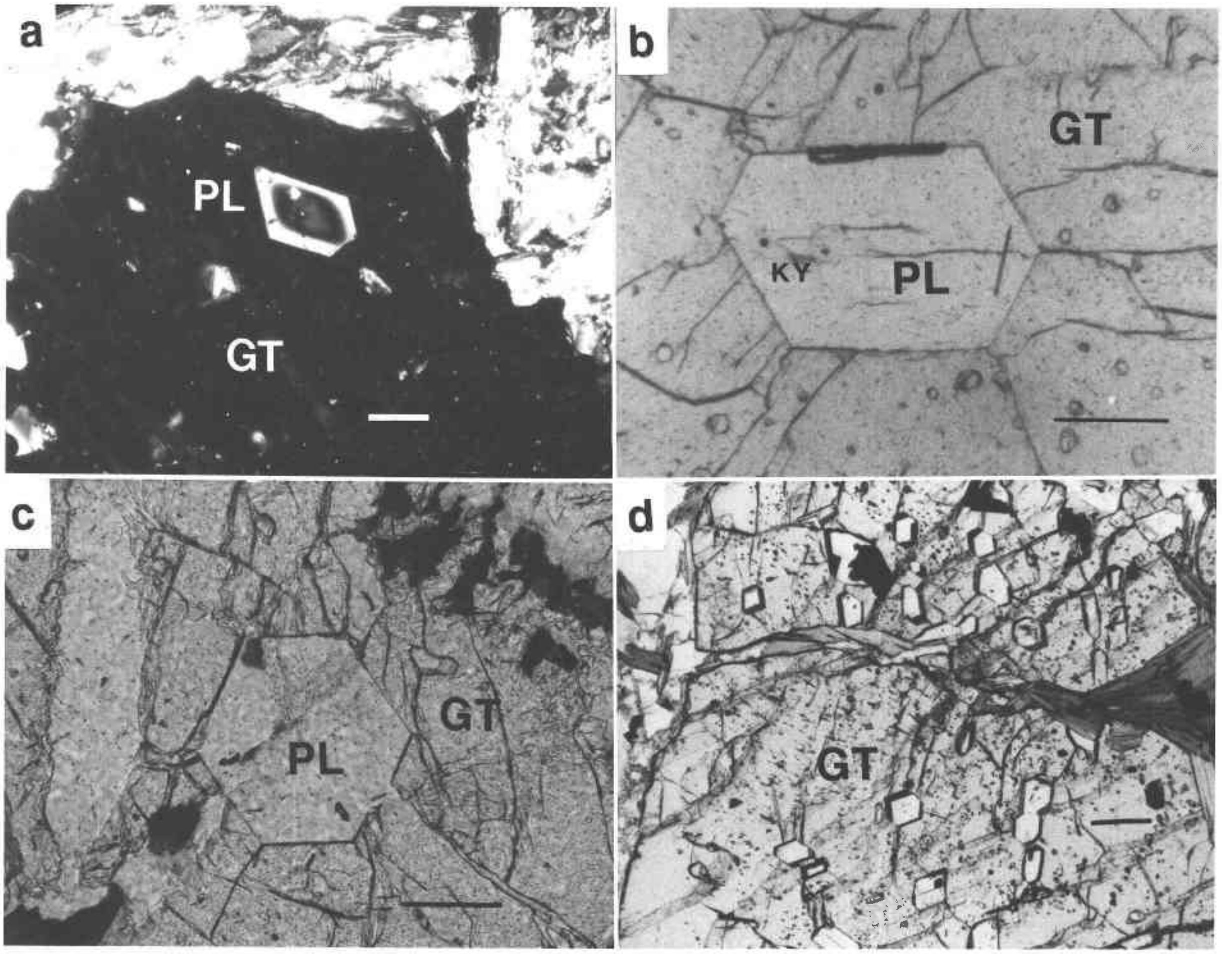

Fig. 1. Photomicrographs of plagioclase inclusions in garnet. All scale bars = 100 μm. GT = garnet; PL = plagioclase; KY = kyanite. (**a**) Faceted plagioclase inclusion in garnet (crossed nicols): SK-2a. (**b**) Faceted plagioclase inclusion in garnet: SK-2b. (**c**) Hexagonal-shaped plagioclase inclusion: SK-2b. (**d**) Faceted plagioclase inclusions in garnet illustrating consistent alignment of faces: SK-2b.

isothermal from 9 to ~5 kbar (Whitney and McGroder, 1989). Pressures were estimated using garnet-Al_2SiO_5-plagioclase-quartz (GASP), garnet-rutile-Al_2SiO_5-ilmenite-quartz (GRAIL), garnet-rutile-ilmenite-plagioclase-quartz (GRIPS), and garnet-cordierite geobarometers. Temperatures were determined by garnet-biotite and garnet-cordierite geothermometry. The thermobarometric results are consistent with interpretation of petrogenetic grids for mineral assemblages in metapelitic and meta-ultramafic rocks in the Skagit Gneiss.

Sample descriptions

Zoned plagioclase inclusions in garnet are present in rocks from both of two known sillimanite-bearing outcrops in the Skagit Gneiss (localities 1s and 2s in Whitney and McGroder, 1989). Plagioclase inclusions in garnet are not abundant in rocks from locality 1s and, when present, are slightly to moderately zoned. These inclusions are faceted, but well-developed crystal shapes are rare. Abundant, strongly zoned, and faceted plagioclase inclusions are present in garnets from locality 2s; these inclusions are the focus of the present investigation.

Thermobarometric estimates indicate that rocks from both sillimanite gneiss outcrops experienced the same *P-T* conditions. The differences in degree of development of zoning and crystal shape noted above may be attributed in part to the greater degree of fracturing of garnets in rocks from locality 2s as compared to garnets from locality 1s (see below).

For this investigation, two samples from locality 2s were studied in detail. Garnet grains in one sample (SK-2a) have an average diameter of 2–3 mm; grains from the second sample (SK-2b) have an average diameter of 5–7 mm. Garnet in both samples has compositionally homogeneous cores in areas away from plagioclase but contains abundant plagioclase inclusions. In addition, garnet crystals are pervasively fractured and have resorbed, partially embayed rims.

Most plagioclase inclusions are faceted, visibly zoned, four- to six-sided crystals (Figs. 1a, 1b), and some have nearly perfect hexagonal shape (Fig. 1c). Because the facets of the plagioclase grains show common orientations in each garnet (Fig. 1d) and are parallel to planes of rutile exsolution in the garnet in sample SK-1, the facets are interpreted as garnet crystal faces, i.e., the plagioclase inclusions are negative crystals.

The maximum metamorphic conditions recorded by these rocks exceeded the stability limit of staurolite in quartz-bearing rocks. Staurolite is, however, preserved as an armored relic in garnet in samples from locality 1s (sample designation SK-1) but is not observed in garnet from the sillimanite gneiss that is the focus of this study (SK-2). The absence of abundant fractures in garnet in SK-1 apparently allowed the preservation of the relict staurolite, but any staurolite that was formerly included in garnet in SK-2 may have reacted with matrix quartz via fractures in garnet. These observations are consistent with differences in development of zoning and negative crystal shape in plagioclase inclusions in the two samples as noted above. Inferences about garnet in SK-1 rest on the assumption that during high-grade metamorphism the garnet did not contain a significant number of fractures that have subsequently healed.

Fractures in the garnet in this study may be classified into three categories: (1) rare, healed fractures that can be detected only in back-scattered electron (BSE) images, (2) fractures that follow a consistent orientation at steep angles to foliation in all garnet within a thin section, and (3) fractures that extend from the corners of faceted plagioclase inclusions at ~90 °C to the inclusions. Calculation of $(\Delta V_{gt} - \Delta V_{plag})/\Delta P$ for pressures from 9 to 5 kbar using data compiled in Berman (1988) shows that the latter type of fracture may have resulted from the expansion of plagioclase relative to garnet during decompression.

Mineral compositions and zoning

Plagioclase and garnet were analyzed with a JEOL 733 Superprobe at the University of Washington using a 15 kV accelerating voltage. Plagioclase was analyzed with a 15 nA sample current. The beam was defocused to minimize Na loss, but was still 2–3 μm in diameter to allow multiple analyses of the smallest inclusions.

Garnet

Changes in garnet composition in the vicinity of plagioclase inclusions can be seen in microprobe line scans of garnet cores (Fig. 2), in BSE images (Fig. 3), and in composition maps of garnet (Fig. 4). The grossular (Ca) content of garnet cores is constant (~10–12 mol%) except in the vicinity of plagioclase inclusions, where it decreases to 3–8 mol% (Figs. 2, 4A, 4D; Table 1). Garnet rims contain ~4–6 mol% grossular.

Almandine (Fe), pyrope (Mg), and spessartine (Mn) abundances are nearly constant in the garnet cores, but vary in the vicinity of plagioclase inclusions (Figs. 2, 4B, 4C). In SK-2a, Fe and Mg increase slightly and Mn remains constant around plagioclase inclusions (Fig. 2A); in SK-2b, Fe and Mn increase and Mg decreases near the plagioclase inclusions (Fig. 2B).

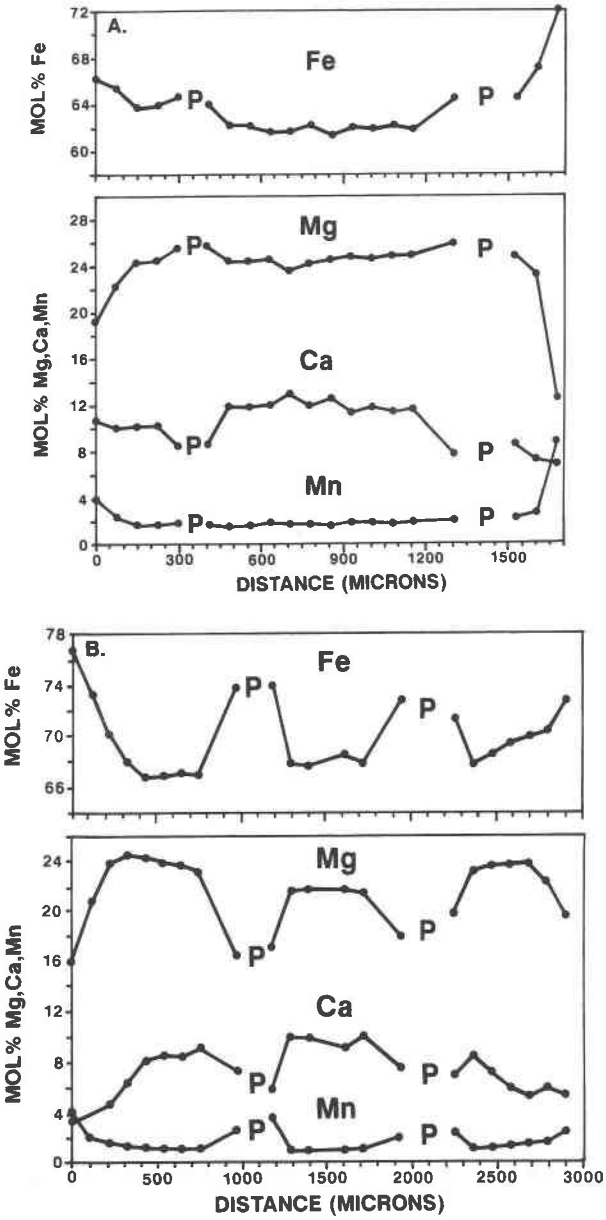

Fig. 2. Garnet zoning profiles. P = plagioclase. (**A**) SK-2a. Microprobe traverse intersects two plagioclase inclusions: the zoning profile for the inclusion on the left is shown in Figure 5b. Zoning around the inclusion on the right is disrupted because of extensive fracturing and the proximity of the inclusion to the garnet rim. (**B**) SK-2b.

Changes in garnet composition around plagioclase inclusions in SK-2b are similar in trend and magnitude to the zoning pattern at garnet rims (Fig. 2). The increase in Mn and Mg and decrease in Fe and Ca at garnet rims is consistent with the interpretation that rim zoning is caused by involvement of garnet in retrograde reactions with fer-

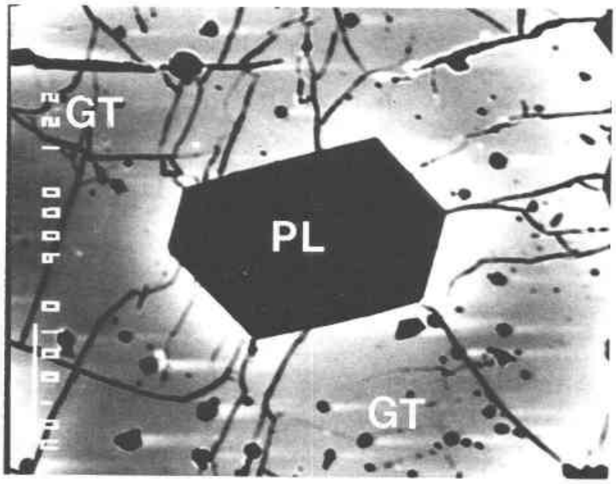

Fig. 3. Back-scatter electron image showing a compositional halo around the plagioclase inclusion in Figure 1b. The scale bar = 100 μm. The increase in brightness near the inclusion corresponds to an increase in Fe. The greater intensity of brightness on the right side of the inclusion is an artifact of the imaging technique, as are the bright areas to the right of smaller inclusions.

romagnesian minerals (e.g., biotite) and plagioclase. Ca depletion halos and Fe-Mg-Mn zoning around plagioclase inclusions may also be due to a retrograde process that consumed garnet. Because of the equilibrium

$$\underset{\text{grossular}}{Ca_3Al_2Si_3O_{12}} + \underset{\text{kyanite}}{2Al_2SiO_5} + \underset{\text{quartz}}{SiO_2} = \underset{\text{anorthite}}{3CaAl_2Si_2O_8} \quad (1)$$

(GASP), a decrease in Ca in garnet near plagioclase inclusions suggests that the plagioclase-garnet interactions that produced these features took place during decompression.

Evidence that fractures in garnet, particularly those that directly connect plagioclase inclusions to the garnet rim, may have acted as conduits for transfer of components between matrix phases and inclusions can be seen in maps of grossular, almandine, and spessartine content around inclusions (Fig. 4). A map of the Ca depletion halo around an inclusion from SK-2a (Fig. 4D) illustrates that the extent of zoning around inclusions is spatially related to fractures in the host garnet.

The change in garnet composition in the vicinity of plagioclase inclusions and at garnet rims is imaged by BSE photography (Fig. 3). Enrichment in Fe is indicated by brighter areas on the BSE image.

Other features evident in some BSE images (not pictured) are healed fractures in garnets. Although the clos-

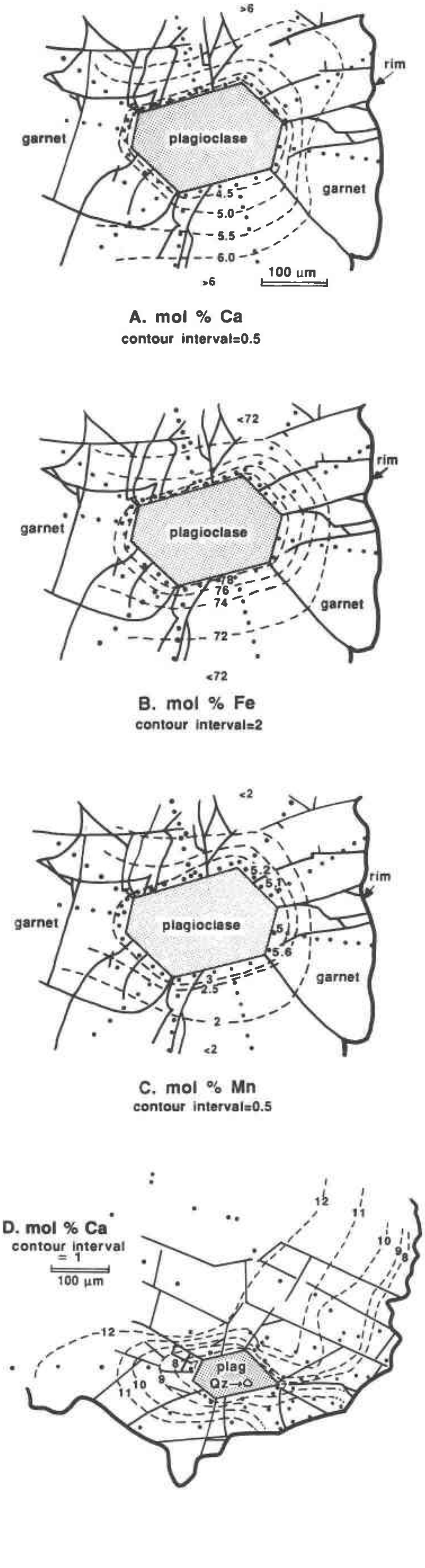

→

Fig. 4. Garnet composition maps. Dots indicate location of microprobe analysis. Dashed lines are contours in mol%; heavy lines indicate fractures in garnet. Rim zoning is not contoured. (**A**) Ca depletion around the inclusion shown in Figures 1b and 3. (**B**) Fe enrichment. (**C**) Mn enrichment. (**D**) Ca depletion around the inclusion in Figure 1a.

TABLE 1. Representative garnet analyses

	SK-2a			SK-2b		
	Core	Rim	Near inclusion	Core	Rim	Near inclusion
SiO_2	38.46	37.51	38.24	37.90	36.77	37.12
TiO_2	0.01	0.02	0.02	0.03	0.07	0.06
Al_2O_3	21.79	21.60	21.44	21.49	21.51	22.45
FeO	28.31	30.58	30.39	30.88	34.36	33.99
MnO	0.69	4.49	0.79	0.49	2.51	2.15
MgO	6.51	3.17	6.96	6.28	2.79	2.81
CaO	4.26	2.71	2.74	2.94	1.64	1.48
Total	100.03	100.08	100.58	100.01	99.66	100.06
			Cations			
Si	3.00	2.92	2.98	2.95	2.97	2.97
Ti	0.00	0.00	0.00	0.00	0.00	0.00
Al	2.00	1.98	1.97	1.97	2.05	2.12
Fe	1.85	1.99	2.01	2.01	2.32	2.27
Mn	0.05	0.30	0.03	0.03	0.17	0.15
Mg	0.76	0.37	0.73	0.73	0.34	0.34
Ca	0.36	0.23	0.25	0.25	0.14	0.13
			Mol%			
Fe	61.45	69.11	64.52	66.64	78.13	78.92
Mn	1.52	10.28	1.70	1.07	5.78	5.06
Mg	25.19	12.77	26.33	24.16	11.31	11.63
Ca	11.85	7.85	7.45	8.13	4.78	4.40

ing of these fractures may predate the interaction between plagioclase inclusions and garnet discussed here, the existence of fossil fractures extends the potential relevance of this study to plagioclase inclusions in garnets that are not now visibly fractured.

Plagioclase

Eighty-six plagioclase inclusions from ten garnets from the two samples were analyzed. Some large inclusions (>100 μm) have homogeneous cores (Fig. 5a); others are more complexly zoned. All inclusions are reversely zoned and most have smooth, continuous zoning profiles (Fig. 5b).

Zoning, viewed optically, parallels plagioclase-garnet interfaces in both faceted and irregularly shaped inclusions, indicating that plagioclase zoning results from reaction between plagioclase and garnet and is not a preentrapment feature. Plagioclase zoning cannot be the result of interdiffusion of CaAl-NaSi within each inclusion because the inclusions are surrounded not only by Ca depletion halos but also by Fe-Mn-Mg zoning in an otherwise homogeneous garnet. Zoning in garnet around plagioclase inclusions is additional evidence that plagioclase zoning is related to interaction between the inclusions and the host garnet.

Plagioclase inclusions analyzed are generally more calcic than matrix plagioclase (An_{22-31}) in the same thin section (Table 2), although some larger inclusions are more sodic than plagioclase in the matrix. Matrix plagioclase is generally homogeneous, though some grains exhibit slight reverse zoning at the rim (Fig. 5c).

Microprobe analyses of inclusion rims document the extent of postentrapment reaction between inclusion and host. Rims of inclusions (i.e., adjacent to the garnet) have

TABLE 2. Representative plagioclase analyses (SK-2b)

		Inclusions in garnet					
		A**		B		C	
	Matrix*	Rim	Core	Rim	Core	Rim	Core
SiO_2	60.68	58.37	63.07	56.54	60.46	54.33	58.32
Al_2O_3	24.91	26.47	23.46	28.34	25.19	28.96	26.25
FeO	0.04	0.04	0.00	0.20	0.00	0.00	0.02
CaO	6.45	7.50	4.50	9.69	6.15	11.50	8.27
Na_2O	7.94	7.08	9.17	5.83	7.97	5.18	6.97
K_2O	0.10	0.08	0.15	0.08	0.11	0.05	0.06
Total	100.12	99.54	100.35	100.68	99.88	100.02	99.89
			Cations				
Si	2.70	2.62	2.78	2.52	2.69	2.45	2.61
Al	1.30	1.40	1.22	1.49	1.32	1.54	1.38
Fe	0.00	0.00	0.00	0.01	0.00	0.00	0.00
Ca	0.31	0.36	0.21	0.46	0.29	0.56	0.40
Na	0.68	0.62	0.78	0.50	0.69	0.45	0.60
K	0.01	0.00	0.01	0.00	0.01	0.00	0.00
An%	30.81	36.75	21.15	47.65	29.71	54.94	39.47

* Analysis is the average of 18 points.
** Inclusion diameters: A = 248 μm; B = 173 μm; C = 78 μm.

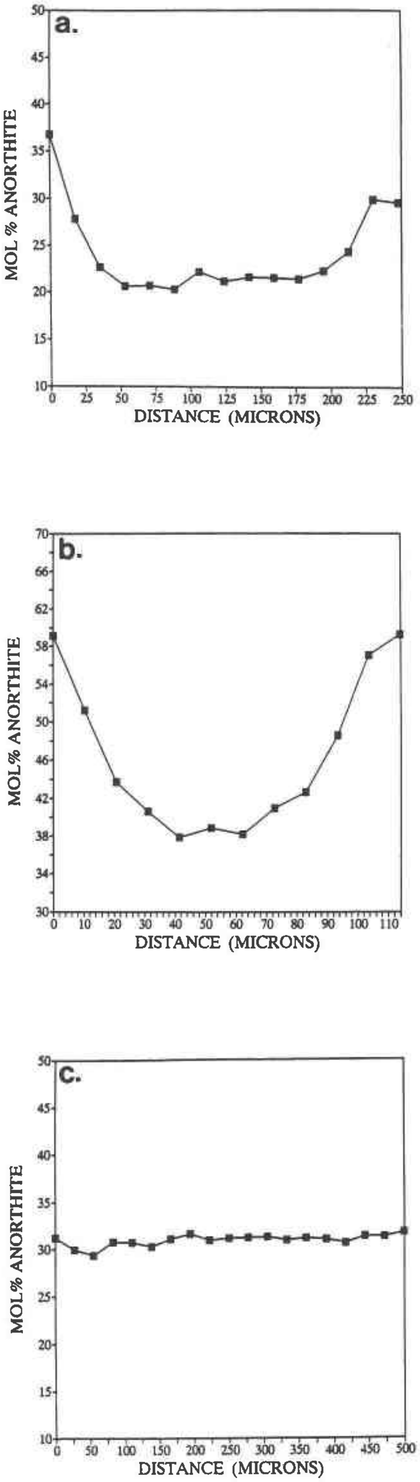

Fig. 5. Plagioclase inclusion zoning profiles. Each profile represents compositional change across the shortest visible dimension of the inclusion. (**a**) SK-2b. The relatively homogeneous core is typical of inclusions >100 μm. (**b**) SK-2a (also see Figs. 1a, 4D). (**c**) SK-2a. Representative zoning profile of matrix plagioclase.

compositions ranging from An_{34} to An_{60}; anorthite content increases from 12 to 24 mol% from core to rim. Core compositions of plagioclase inclusions range from An_{16} to An_{36}.

Because the inclusions are zoned, the anorthite content of each inclusion core is a function of the distance from the plagioclase-garnet interface at which the plane of the thin section surface intersects the inclusion. If the inclusions are approximately equant, most of the smallest inclusions could represent slices through plagioclase near the inclusion-garnet interface, and these inclusions would thus be the most calcic. Based on an examination of 45 inclusions from garnet in SK-2b, it can be seen that inclusion size can be correlated with anorthite content (Fig. 6). This suggests that although the cores of inclusions >200 μm may represent relict compositions, the anorthite content of inclusions that appear small in thin section may actually represent rim compositions. Alternatively, if the correlation between size and anorthite content is not just an artifact of the thin sectioning "cut effect," the observed trend may indicate that the compositions of small inclusions have been entirely modified by reaction with the host garnet. Whether the relation between apparent size and anorthite content is an artifact or represents a correlation between actual inclusion size and composition, the significance of this observation is that the results of geobarometric calculations will differ not only as a function of the location of the microprobe analysis on the plagioclase grain (core vs. rim), but also of the apparent size of the inclusion analyzed.

Discussion

Reactions

Plagioclase inclusions in garnet could only have changed composition by a net transfer reaction if they were able to incorporate components from matrix phases (e.g., Al_2SiO_5 and quartz). This suggests that the inclusions reacted with host garnets by communicating with matrix minerals via fractures in the garnet. As noted above, garnet-plagioclase reaction most likely took place during decompression.

Because of its central role in geobarometric calculations for pelitic rocks, the net-transfer GASP Reaction 1 has been the only equilibrium considered thus far in this discussion. In view of the fact that communication between plagioclase inclusions and matrix phases may have involved transport of components in a fluid, and because a large number of plagioclase inclusions in these samples contain inclusions of kyanite and quartz (see below), it is also useful to consider reactions of the form

$$\underset{\text{grossular}}{2Ca_3Al_2Si_3O_{12}} = \underset{\text{kyanite}}{Al_2SiO_5} + \underset{\text{anorthite}}{CaAl_2Si_2O_8} + \underset{\text{quartz}}{3SiO_2} + 5CaO_{(aq)} \quad (2)$$

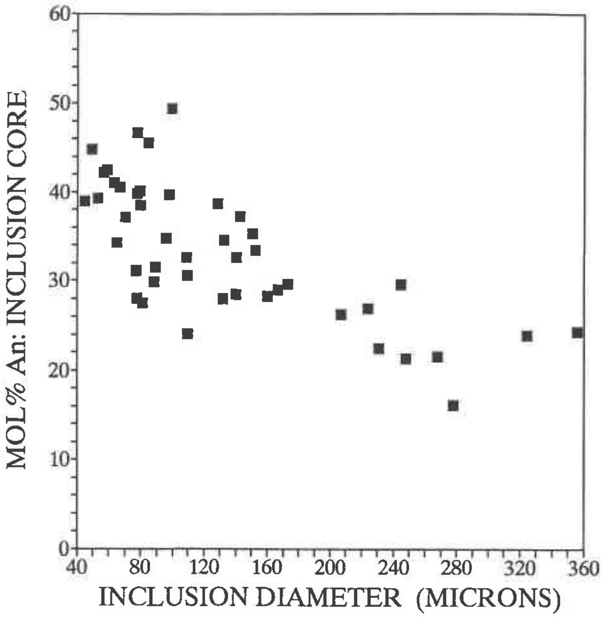

Fig. 6. Mol% An of the centers of 45 inclusions from garnet grains in SK-2b plotted against inclusion diameter (shortest visible dimension). Scatter in the data reflects the influence on anorthite content of the cut effect (see text) and of the number and size of cracks surrounding each inclusion.

which can also be written as a hydrolysis reaction:

$$2Ca_3Al_2Si_3O_{12} + 10H^+ = Al_2SiO_5 + CaAl_2Si_2O_8 + 3SiO_2 + 5Ca^{2+} + 5H_2O. \quad (3)$$

These reactions differ from Reaction 1 in that aluminosilicate and quartz are products in Reactions 2 and 3, and the sign of the volume change is opposite to that of the GASP reaction. Other reactions involving plagioclase, almandine-pyrope components in garnet, and biotite can be written that consume Ca and Si and liberate H^+ and K^+.

Reactions 2 and 3 describe the interaction of garnet with a pore fluid to produce aluminosilicate, quartz, and anorthite component. Possible textural evidence for this reaction is the presence of small grains of kyanite and quartz in many of the plagioclase inclusions (Figs. 1a, 4D, 7a). It is not possible to determine whether the kyanite and quartz are relict matrix phases or products of garnet-plagioclase reaction, but if they are postentrapment reaction products, the fact that the aluminosilicate phase is kyanite and not sillimanite indicates that reaction took place near the maximum pressure conditions recorded (Whitney and McGroder, 1989).

The presence of islands of garnet in some plagioclase inclusions is evidence that these inclusions grew at the expense of the host garnet (Fig. 7b). It is interesting to speculate that some of the inclusions may have grown entirely as a result of reaction between garnet and a pore fluid and are not, therefore, included former matrix phases.

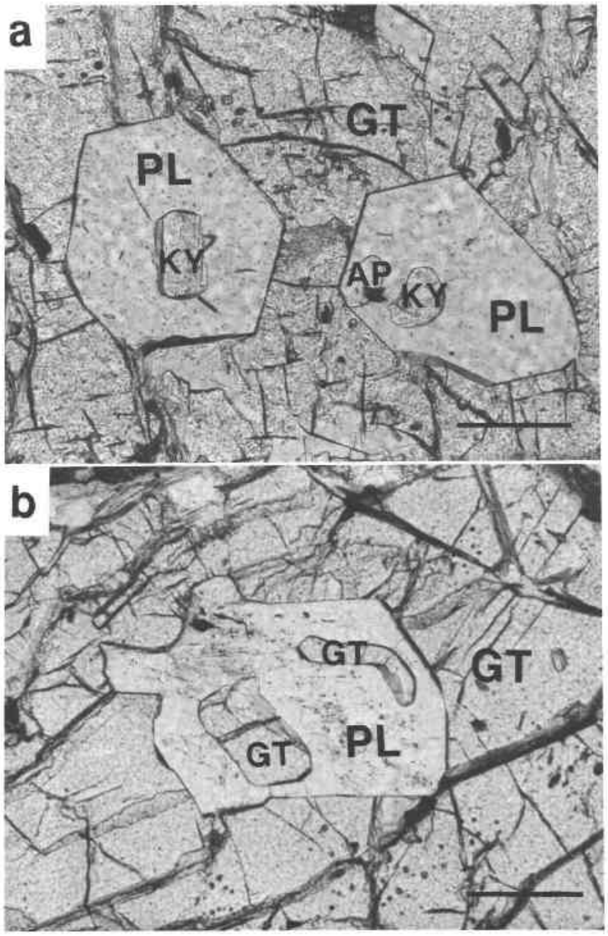

Fig. 7. Photomicrographs of plagioclase inclusions in garnet. All scale bars = 100 μm. GT = garnet; PL = plagioclase; KY = kyanite; AP = apatite. (**a**) Kyanite in a plagioclase inclusion in garnet. (**b**) Remnant garnet islands in a plagioclase inclusion in garnet.

Conclusions

Interpretations, related observations, and conclusions include:

1. A free fluid may have been present at some time during the decompression phase of the high-grade metamorphism. A pore fluid acting as the medium of mass transport between inclusions and matrix would have facilitated reaction(s). The complex fluid history of these rocks will be discussed elsewhere as part of a study of the migmatization of the Skagit Gneiss.

2. Although the features documented here are unusual, they are not unique. Reversely zoned, faceted plagioclase inclusions with rims as calcic as An_{95} are present in garnet in a sillimanite gneiss from the Ladakh region of Pakistan (M.U.K. Khattak, personal communication, 1990).

3. The interpretations presented above are based on a

study of minerals in a high-grade pelitic gneiss, but these results may also be applicable to rocks of other lithologies (e.g., amphibolites) that contain plagioclase inclusions in garnets (S.M. Kuehner, personal communication, 1990).

4. The use of plagioclase inclusions in garnet for the construction of quantitative *P-T* paths may give erroneous results. Interpretation of geobarometric results that utilize plagioclase inclusions in garnet must allow for the possibility that plagioclase inclusions have changed composition after entrapment in garnet. It is not sufficient to assume that plagioclase inclusions have been effectively armored by the host garnet without testing the validity of this assumption by looking for systematic zoning patterns in inclusion and host. The test is facilitated when the plagioclase inclusions are fairly large (>40 μm).

Pressures calculated for the Skagit rocks with the GASP geobarometer (Ghent, 1976; Newton and Haselton, 1981) using garnet core and plagioclase inclusion core compositions are 2.5–4.4 kbar higher than pressures calculated using plagioclase inclusion rim and adjacent garnet compositions. Although the absolute pressures calculated are undefined unless *T* is known, the magnitude of this pressure difference is an indication of the error that may be introduced into geobarometric determinations using plagioclase inclusions in garnet.

This study demonstrates that plagioclase inclusions in garnet may not be chemically isolated from reaction with matrix phases if fractures in the host garnet act as conduits for mass transfer at sufficiently high temperatures for a reaction to proceed. Care must be taken when using plagioclase inclusions in garnet in high-grade metamorphic rocks for geobarometric calculations and construction of quantitative *P-T* paths. It is not the intention of this paper to dismiss all pressures obtained using plagioclase inclusions, but to note that the assumption that plagioclase inclusions in garnet do not change composition after entrapment may be invalid if the garnet was fractured during metamorphism.

Acknowledgments

Critical reviews by Tom Hoisch, Jeff Grambling, Ed Young, Bernard Evans, and Marc Hirschmann significantly improved this paper. Scott Kuehner provided invaluable microprobe assistance and interesting discussions about plagioclase inclusions.

References cited

Berman, R.G. (1988) Internally-consistent thermodynamic data for stoichiometric minerals in the system Na_2O-K_2O-CaO-MgO-FeO-Fe_2O_3-Al_2O_3-SiO_2-TiO_2-H_2O-CO_2. Journal of Petrology, 29, 445–522.

Ghent, E.D. (1976) Plagioclase-garnet-Al_2SiO_5-quartz: A potential geobarometer-geothermometer. American Mineralogist, 61, 710–714.

Lieberman, J.E. (1988) Metamorphic and structural studies of the Kigluaik Mountains, western Alaska, 191 p. Ph.D. thesis, University of Washington, Seattle, Washington.

Loomis, T.P. (1983) Compositional zoning of crystals: A record of growth and reaction history. In S.K. Saxena, Ed., Kinetics and equilibrium in mineral reactions, p. 1–60. Springer-Verlag, New York.

Newton, R.C., and Haselton, H.T. (1981) Thermodynamics of the garnet-plagioclase-Al_2SiO_5-quartz geobarometer. In R.C. Newton, A. Navrotsky, and B.J. Wood, Eds., Thermodynamics of minerals and melts, p. 129–145. Springer-Verlag, New York.

Spear, F.S. (1989) Petrologic determination of metamorphic pressure-temperature-time paths. In F.S. Spear and S.M. Peacock, Eds., Metamorphic pressure-temperature-time paths, International Geologic Congress, Short Course vol. 7, p. 1–56. American Geophysical Union, Washington, D.C.

Spear, F.S., and Rumble, D. (1986) Pressure, temperature, and structural evolution of the Orfordville belt, west-central New Hampshire, Journal of Petrology, 27, 1071–1093.

Spear, F.S., and Selverstone, J. (1983) Quantitative P-T paths from zoned minerals: Theory and tectonic applications. Contributions to Mineralogy and Petrology, 83, 348–357.

St. Onge, M.R. (1987) Zoned poikiloblastic garnets: P-T paths and synmetamorphic uplift through 30 kilometers of structural depth, Wopmay orogen, Canada. Journal of Petrology, 28, 1–21.

Whitney, D.L., and McGroder, M.F. (1989) Cretaceous crustal section through the proposed Insular-Intermontane suture, North Cascades, Washington. Geology, 17, 555–558.

Manuscript received May 3, 1990
Manuscript accepted January 14, 1991